Analytical Improvement on the Electromagnetic Scattering From Deformed Spherical Conducting Objects

Baris Ates, Alp Kustepeli, and Zebih Cetin

***Abstract*— In this article, electromagnetic scattering from conducting deformed spheres is considered analytically by employing the perturbation method and utilizing Debye potentials. To be able to analyze a wide variety of scattering problems, azimuthal variation is indispensable, and therefore, the geometries of the scatterers considered in this study do not have rotational symmetry; hence, they are dependent on the θ and φ angles in spherical coordinates. Analyses are carried up to the second order explicitly to obtain more accurate results, and thus, scattered fields are obtained with second-order corrections. The coefficients used to determine the scattered field are expressed in terms of Clebsch–Gordan coefficients, which enables one to obtain the results for new geometries only by simple algebraic manipulations. Numerical results and their comparisons are also presented for various deformation functions and parameters.**

***Index Terms*— Analytical solution, Debye potential, electromagnetic wave scattering, perturbation method (PM), radar cross section (RCS).**

I. Introduction

NONSPHERICAL objects are of great importance and taken into consideration in many areas of study, e.g., elasticity [1], fluid dynamics [2], neuroscience [3], astrophysics [4], and acoustics [5]–[7], including electromagnetic scattering [8], [9]. The interest in the scattering properties of conducting objects for real-life problems [10]–[13] never decreases for researchers in many different fields [14]–[16]. The studies on PEC bodies maintain their importance because they either find direct applications [17], [18] or allow one to examine and understand more complex materials, such as dielectrics and others [7], [19]–[22]. One of the realistic examples of those dielectric objects is raindrop, which causes attenuation [23]. Even though raindrops are assumed as spherical in shape in the analysis [24], because of the gravity, wind, pressure, and other effects, they actually differ much and their shapes deviate from the sphere. To determine the shape of raindrop, several successful models have been developed [25], [26] and the results show that the sphericity assumption is not very satisfactory for realistic calculations if its size is large [27], [28].

Since the exact solution to electromagnetic scattering problems can be obtained only for certain geometries [26], many methods have been developed and applied for the detailed investigation of scattering by any object, e.g., the perturbation method (PM) [29], [30], the point matching method [31], the method of moments [32], [33], the generalized multipole method [34], the volume integral equation method [35], the finite-difference time-domain method [36], the finite-element method [37], the T matrix method [38], and the Sh matrix method [39]. Although numerical methods are very valuable and utilizable, the superiority of analytical methods in many aspects, such as completeness, accuracy, time, and memory requirements, is greatly appreciated, and therefore, they are much more preferred [40], [41].

The PM [29], [42]–[44] can be considered as an advantageous one since a full analytic approach is employed. The method was employed up to the first order for various important obstacles having rotational symmetry [29], [45], [46]. However, even for very specific geometries and problems, lower order calculations are not sufficient for accurate results [47]–[50] and to reveal the physics behind as well [5]–[22], [46], [51]–[55]. Therefore, the order of the method turns out to be very important for a clear and deep understanding of more complicated problems. Even though there were some attempts to increase the order to obtain more accurate results for scatterers having arbitrary geometries, due to the complexity of the integrals involved, only the general theory with the closed form of the integrals was presented without their evaluation [29], [43], [56].

The geometries considered in this work are obtained by the smooth deformations of sphere which are dependent on both θ and φ angles in spherical coordinates. In addition to this, instead of the statistical version of the PM that causes loss of information [57]–[59], the problem is examined directly by using the second-order perturbation theory and neither averaging methods nor additional assumptions are used, such as in [60]–[62]. In this sense, present work could be regarded as a generalization of [63].

Vector wave functions are commonly used to express the fields [29], [43], [44], [57], [59], [64], [65], but since it is

Manuscript received January 17, 2021; accepted May 11, 2021. Date of publication July 16, 2021; date of current version December 16, 2021. *(Corresponding author: Baris Ates.)*

Baris Ates was with the Department of Mathematics, İzmir Institute of Technology, Urla 35430, Turkey. He is now with the Ministry of National Education, 35380 Buca, Turkey (e-mail: baristes2002@gmail.com).

Alp Kustepeli is with the Department of Electrical and Electronics Engineering, İzmir Institute of Technology, 35430 Urla, Turkey (e-mail: alpkustepeli@iyte.edu.tr).

Zebih Cetin is with the Department of Physics, İzmir Institute of Technology, 35430 Urla, Turkey (e-mail: zebihcetin@iyte.edu.tr).

Color versions of one or more figures in this article are available at https://doi.org/10.1109/TAP.2021.3096317.

Digital Object Identifier 10.1109/TAP.2021.3096317

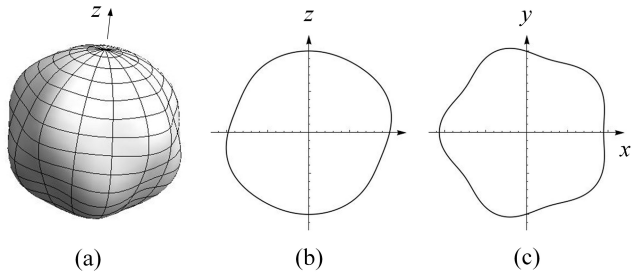

Fig. 1. Geometry obtained by deformation functions $f_1(\theta,\varphi) = \mathrm{Re}(Y_6^5(\theta,\varphi))$ and $f_2(\theta,\varphi) = \mathrm{Re}(Y_6^6(\theta,\varphi))$. (a) 3-D geometry. (b) θ variation for $\varphi = \pi/6$. (c) φ variation for $\theta = \pi/3$.

easier to deal with one function than three, scalar functions are considered instead of vector functions, and hence, Debye potentials are utilized. Spherical harmonic expansion is also utilized to expand the deformation functions in terms of spherical harmonics denoted by $Y_n^m(\theta,\varphi)$ [66], which enables one to obtain the results for new geometries very easily without repeating all of the calculations and to examine any scatterer under TE or TM incidence without any additional, special, or separate treatment through Wigner rotation matrices. The unknown coefficients used to represent the scattered field are presented explicitly and all of the surface integrals involved are evaluated analytically.

II. Formulation and Solution

Geometries of the scatterers considered in this study are obtained by small and smooth deformations of spheres and their surfaces are described in spherical coordinates by

$$r = r_s(\theta,\varphi) = R(1 + \beta f_1(\theta,\varphi) + \beta^2 f_2(\theta,\varphi)) \tag{1}$$

where r, θ, and φ are the spherical coordinates, R represents the radius of the sphere to be perturbed, β is the small perturbation parameter, and $f_1(\theta,\varphi)$ and $f_2(\theta,\varphi)$ are arbitrary deformation functions. One of the θ- and φ-dependent geometries to be examined can be seen in Fig. 1 and it is obtained using the real parts of the spherical harmonics for the deformation functions where Re() represents the real part. The total electric field $\vec{E} = \vec{E}^{\mathrm{i}} + \vec{E}^{\mathrm{s}}$ where $\vec{E}^{\mathrm{i}}$ and $\vec{E}^{\mathrm{s}}$ are the incident and scattered fields, respectively, and for the perturbed case, it can be written in terms of the perturbation parameter β as [29]

$$\vec{E}(r,\theta,\varphi) = \vec{E}_0 + \beta\vec{E}_1 + \beta^2\vec{E}_2 + O(\beta^3) \tag{2}$$

where $\vec{E}_0(r,\theta,\varphi)$ is the field component for the sphere and it corresponds to the zeroth-order solution, $\vec{E}_1(r,\theta,\varphi)$ is the contribution from the first-order correction, and finally, $\vec{E}_2(r,\theta,\varphi)$ is the contribution due to the second-order correction. By the formulation given in (2), it can be concluded that the field for the deformed sphere is obtained by the summation of the field belonging to the sphere together with the first- and second-order corrections. Although the complexity of the calculations increases enormously due to the increase in the order of PM especially when the φ dependence is taken into consideration to be able to represent an arbitrary geometry for the scatterer, analyses are carried up to the second order to obtain more accurate results. The time dependence is assumed to be $e^{-i\omega t}$ and suppressed throughout this article ($i = \sqrt{-1}$). The scattered field components are of the forms [67]

$$\begin{aligned}
E_{\gamma r} &= \sum_{m,n} \frac{i a_{\gamma mn}}{\omega\mu\epsilon} Z_{1n}(kr) P_n^m(\cos\theta) e^{im\varphi} \\
E_{\gamma\theta} &= \sum_{m,n} \frac{i a_{\gamma mn}}{\omega\mu\epsilon} Z_{2n}(kr) \frac{d}{d\theta} P_n^m(\cos\theta) e^{im\varphi} \\
&\quad - \sum_{m,n} \frac{im}{\epsilon \sin\theta} b_{\gamma mn} Z_{3n}(kr) P_n^m(\cos\theta) e^{im\varphi} \\
E_{\gamma\varphi} &= -\sum_{m,n} \frac{m a_{\gamma mn}}{\omega\mu\epsilon \sin\theta} Z_{2n}(kr) P_n^m(\cos\theta) e^{im\varphi} \\
&\quad + \sum_{m,n} \frac{b_{\gamma mn}}{\epsilon} Z_{3n}(kr) \frac{d}{d\theta} P_n^m(\cos\theta) e^{im\varphi}
\end{aligned} \tag{3}$$

where $\sum_{m,n} = \sum_{n=1}^{\infty}\sum_{m=-n}^{n}$ and γ indicates the order of perturbation. The Z functions seen in (3) are $Z_{1\,n}(kr) = ((d^2/dr^2) + k^2)(kr\, h_n^{(1)}(kr))$, $Z_{2\,n}(kr) = (1/r)(d/dr)(kr\, h_n^{(1)}(kr))$, and $Z_{3\,n}(kr) = k\, h_n^{(1)}(kr)$ and $h_n^{(1)}$ is the spherical Hankel function of the first kind. P_n^m is the associated Legendre function [66], k is the wavenumber of the surrounding medium, ϵ is the permittivity, and μ is the permeability. The coefficients $a_{\gamma mn}$ and $b_{\gamma mn}$ are arbitrary constants [9], [67] and they are determined by using the boundary condition on the surface of the conductor, $\hat{n} \times \vec{E}|_{r=r_s} = 0$, where $\hat{n}$ is the unit normal vector on the surface and it is described up to the second order by

$$\begin{aligned}
\hat{n} &= \left(1 - \beta^2\left(\frac{1}{2}\left(\frac{\partial f_1}{\partial\theta}\right)^2 + \frac{1}{2\sin^2\theta}\left(\frac{\partial f_1}{\partial\varphi}\right)^2\right)\right)\hat{r} \\
&\quad + \left(-\beta\frac{\partial f_1}{\partial\theta} + \beta^2 f_1\frac{\partial f_1}{\partial\theta} - \beta^2\frac{\partial f_2}{\partial\theta}\right)\hat{\theta} \\
&\quad + \left(-\beta\frac{1}{\sin\theta}\frac{\partial f_1}{\partial\varphi} + \beta^2\frac{f_1}{\sin\theta}\frac{\partial f_1}{\partial\varphi} - \beta^2\frac{1}{\sin\theta}\frac{\partial f_2}{\partial\varphi}\right)\hat{\varphi} \\
&\quad + O(\beta^3).
\end{aligned} \tag{4}$$

Considering r_s in (1) as $r_s = R + \Delta R$ where $\Delta R = \beta f_1 R + \beta^2 f_2 R$, the expressions for the field components up to the second order are obtained as

$$\begin{aligned}
E_{\gamma\alpha}(r_s,\theta,\varphi) &= E_{\gamma\alpha}(R + \Delta R,\theta,\varphi) \\
&= \Bigg[E_{\gamma\alpha}(r,\theta,\varphi) + \beta f_1 r\frac{\partial}{\partial r}E_{\gamma\alpha}(r,\theta,\varphi) \\
&\quad + \beta^2 f_2 r\frac{\partial}{\partial r}E_{\gamma\alpha}(r,\theta,\varphi) + \frac{\beta^2(f_1)^2 r^2}{2} \\
&\quad \times \frac{\partial^2}{\partial r^2}E_{\gamma\alpha}(r,\theta,\varphi)\Bigg]_{r=R} + O(\beta^3)
\end{aligned} \tag{5}$$

where α indicates the r, θ, or φ component of the fields in spherical coordinates.

A. Scattering From Conducting Sphere; Zeroth-Order Solution

To employ the PM, one must first obtain the zeroth-order solution, which corresponds to the plane wave scattering by a

conducting sphere. Considering (2), the total electric field for the zeroth-order solution can be represented as $\vec{E} = \vec{E}^{\mathrm{i}} + \vec{E}^{\mathrm{s}} = \vec{E}_0$, and in this case, $\vec{E}^s = \vec{E}^{\mathrm{sph}}$ and, therefore, $\vec{E}_0 = \vec{E}^{\mathrm{i}} + \vec{E}^{\mathrm{sph}}$, where $\vec{E}^{\mathrm{i}}$ is the incident field and $\vec{E}^{\mathrm{sph}}$ is the scattered field from the sphere. If the incident field is considered as $\vec{E}^{\mathrm{i}} = E^{\mathrm{i}} e^{ikz}\hat{x}$ where E^{i} is an arbitrary constant, it can be expressed in spherical coordinates by the expansion [68]

$$\vec{E}^{\mathrm{i}} = E^{\mathrm{i}} \sum_{n=0}^{\infty} a_n \Bigg[-i \frac{\cos\varphi}{kr} j_n(kr) P_n^1(\cos\theta)\hat{r} + \cos\theta\cos\varphi\, j_n(kr) P_n^0(\cos\theta)\hat{\theta} - \sin\varphi\, j_n(kr) P_n^0(\cos\theta)\hat{\varphi} \Bigg] \tag{6}$$

where $a_n = i^n(2n+1)$ and j_n is the spherical Bessel function of the first kind. The incident field can also be expressed in terms of the representation given in (3) by arranging the coefficients and using j_n for the Z functions accordingly. Thus, the unknown coefficients $a_{0\ mn}$ and $b_{0\ mn}$ to be used to determine the scattered field can be obtained as

$$a_{0\ mn} = \begin{cases} E^{\mathrm{i}} \dfrac{i^n(2n+1)(kRj_n(kR))'}{2\omega n(n+1)(kRh_n^{(1)}(kR))'}, & m = 1 \\ -E^{\mathrm{i}} \dfrac{i^n(2n+1)(kRj_n(kR))'}{2\omega(kRh_n^{(1)}(kR))'}, & m = -1 \\ 0, & m \neq \pm 1 \end{cases} \tag{7}$$

$$b_{0\ mn} = \begin{cases} E^{\mathrm{i}} \dfrac{-i^{n+1}(2n+1)j_n(kR)}{2\omega\eta n(n+1)h_n^{(1)}(kR)}, & m = 1 \\ -E^{\mathrm{i}} \dfrac{i^{n+1}(2n+1)j_n(kR)}{2\omega\eta h_n^{(1)}(kR)}, & m = -1 \\ 0, & m \neq \pm 1 \end{cases} \tag{8}$$

by using the relations of Legendre functions [66]. The primes in (7) and (8) represent the derivatives with respect to the argument of the functions. η is the intrinsic impedance of the medium.

B. Scattering From Deformed Conducting Sphere—First-Order Corrections

For the first-order corrections, the total field can be written as $\vec{E} = \vec{E}_0 + \beta\vec{E}_1 = \vec{E}^{\mathrm{i}} + \vec{E}^{\mathrm{sph}} + \beta\vec{E}_1$ by neglecting higher order terms in (2), and for this case, the scattered field $\vec{E}^{\mathrm{s}} = \vec{E}^{\mathrm{sph}} + \beta\vec{E}_1$. Considering the angular dependencies of the field defined in (3), it would be very convenient to find and utilize the spherical harmonics expansion of the perturbation function $f_1(\theta,\varphi)$ as [6]

$$f_1(\theta,\varphi) = \sum_{j=0}^{\infty}\sum_{s=-j}^{j} d_j^s Y_j^s = \sum_{j=0}^{\infty}\sum_{s=-j}^{j} f_j^s P_j^s(\cos\theta) e^{is\varphi}. \tag{9}$$

It should be noted here that, for some functions, the summation term j could be infinite; in such a case, summation term must be truncated at a large value in order to make sure that particle's shape is represented accurately [58]. The first-order perturbation coefficients $a_{1\ mn}$ and $b_{1\ mn}$ can be obtained as

$$a_{1mn} = -\Bigg[\frac{\omega\mu\epsilon(2n+1)(n-m)!}{4\pi Z_{2n}(kr)m(n+m)!} \times \Bigg(K_1(m,n) + \sum_{p,q}\sum_{j,s} A_1^q(p,q,j,s,n,m)\ \delta_{qsm} + \sum_{p}\sum_{j,s} A_1(p,j,s,n,m) \Bigg) \Bigg]_{r=R} \tag{10}$$

where

$$K_1(m,n) = \Bigg(\frac{4\pi k b_{1mn+1}(n+m+1)(n+2)}{(2n+3)(2n+1)} h_{n+1}^{(1)}(kr) - \frac{4\pi k b_{1mn-1}(n-1)(n-m)}{(2n-1)(2n+1)} h_{n-1}^{(1)}(kr) \Bigg) \times \frac{(n+m)!}{\epsilon(n-m)!} \tag{11}$$

$$b_{1mn} = \Bigg[\Bigg(\frac{\omega\mu\epsilon(2n+1)(\mathrm{n\text{-}m})!}{4\pi i Z_{1n}(kr)(n+m)!} \Bigg) \times \Bigg(\sum_{p,q}\sum_{j,s} \delta_{qsm} \times B_1^q(p,q,j,s,n,m) + \sum_{p}\sum_{j,s} B_1(p,j,s,n,m) \Bigg) \Bigg]_{r=R} \tag{12}$$

$\delta_{qsm} = 2\pi\delta_{q+s,m}$ and $\delta_{i,j}$ is the Kronecker delta. A_1, A_1^q, B_1, B_1^q, and all the other A and B functions with various indices to be seen below are presented in the Appendix. The superscript q in the A and B functions indicates that those functions are dependent on an additional parameter q and they are related to the scattered fields, while the others are related to the incident field.

C. Scattering From Deformed Conducting Sphere—Second-Order Corrections

To obtain more accurate results, one needs to add more correction terms by considering the higher order solutions, and therefore, it is now intended to determine the field by obtaining the second-order coefficients [9], [53]–[55]. For the second-order corrections, the total field can be written as $\vec{E} = \vec{E}_0 + \beta\vec{E}_1 + \beta^2\vec{E}_2 = \vec{E}^{\mathrm{i}} + \vec{E}^{\mathrm{sph}} + \beta\vec{E}_1 + \beta^2\vec{E}_2$, and in this case, the scattered field $\vec{E}^{\mathrm{s}} = \vec{E}^{\mathrm{sph}} + \beta\vec{E}_1 + \beta^2\vec{E}_2$. Similar to $f_1(\theta,\varphi)$ in (9), it will also be convenient to expand $f_2(\theta,\varphi)$ and $(f_1(\theta,\varphi))^2$ in terms of the spherical harmonics as

$$f_2(\theta,\varphi) = \sum_{j=0}^{\infty}\sum_{s=-j}^{j} h_j^s P_j^s(\cos\theta) e^{is\varphi} \tag{13}$$

$$(f_1(\theta,\varphi))^2 = \sum_{j=0}^{\infty}\sum_{s=-j}^{j} k_j^s P_j^s(\cos\theta) e^{is\varphi}. \tag{14}$$

Considering the field components given in (3) and the spherical harmonics expansions presented in (9), (13), and (14),

using the orthogonality relations [65] and performing the integrals involving multiplication of various forms of three associated Legendre functions given in the Appendix, one can obtain

$$a_{2mn} = -\left[\frac{\omega\mu\epsilon(2n+1)(n-m)!}{4\pi Z_{2n}(kr)m(n+m)!} \times \left(K_2(m,n) + \sum_{p,q}\sum_{j,s}\sum_{\nu=2}^{10} A_\nu^q(p,q,j,s,n,m)\ \delta_{qsm} + \sum_{p}\sum_{j,s}\sum_{\nu=11}^{15} A_\nu(p,j,s,n,m)\right)\right]_{r=R} \tag{15}$$

where

$$K_2(m,n) = \left(\frac{4\pi k b_{2mn+1}(n+m+1)(n+2)}{(2n+3)(2n+1)} h_{n+1}^{(1)}(kr) - \frac{4\pi k b_{2mn-1}(n-1)(n-m)}{(2n-1)(2n+1)} h_{n-1}^{(1)}(kr)\right) \times \frac{(n+m)!}{\epsilon(n-m)!} \tag{16}$$

$$b_{2mn} = \left[\frac{\omega\mu\epsilon(2n+1)(n-m)!}{4\pi i Z_{1n}(kr)(n+m)!} \times \left(\sum_{p,q}\sum_{j,s}\sum_{\nu=2}^{18} \delta_{qsm} \times B_\nu^q(p,q,j,s,n,m) + \sum_{p}\sum_{j,s}\sum_{\nu=19}^{25} B_\nu(p,j,s,n,m)\right)\right]_{r=R}. \tag{17}$$

If a_{1mn} and b_{1mn} presented in (10) and (12), respectively, are taken into consideration with the expressions of the A and B functions given in the Appendix, one may conclude that it can be quite difficult to obtain the first-order corrections if there is a φ variation in the scatterer geometry and it can be noticed that the results can be obtained by using the A and B functions with $\nu = 1$ in those cases. Moreover, the complexity and difficulty of obtaining the second-order corrections for such cases can be well appreciated if one examines (15) and (17) that include all of the A and B functions with $\nu \geq 2$ accordingly.

III. Validation and Numerical Results

In this section, first, the results are verified and validated by comparisons in terms of the radar cross section (RCS) [68]

$$\sigma = \lim_{r\to\infty}\left(4\pi r^2 \frac{|\vec{E}^{\mathrm{s}}|^2}{|\vec{E}^{\mathrm{i}}|^2}\right). \tag{18}$$

Use previously published ones obtained for φ independent scatterers and utilize their transformed forms. Then, more results are presented for θ- and φ-dependent scatterers, e.g., ellipsoids, also called triaxial ellipsoids. Similar to (2), RCS for the perturbed case can also be written as

$$\sigma = \sigma^{\mathrm{sph}} + \beta\sigma_1 + \beta^2\sigma_2 + O(\beta^3) \tag{19}$$

where σ^{sph} corresponds to RCS from the sphere and σ_1 and σ_2 are the first- and second-order corrections, respectively. Actually, the efficiency of the method lies on the fact that, in the PM with the representation given in (19), separation of size and shape of scatterer enables to analyze the results for many new geometries for fixed deformation function but different perturbation parameters without repeating all of the calculations. It is sufficient to change the perturbation parameter and use the previously obtained σ's. This feature of the PM makes it an advantageous one to save time in terms of computations [69]. To employ the PM through the general representation in (2) via the expansions given in (3), the summations seen in (3) must be truncated accordingly in order to achieve a good convergence. Hence, it can be concluded that for the purposes of this study, choosing $N = 15$ is sufficient to obtain satisfactory results regarding the convergence as in [64].

For comparisons and verifications, three different cases are examined. In the first case, the θ- and φ-independent deformation functions $f_1(\theta,\varphi) = C_1$ and $f_2(\theta,\varphi) = C_2$ can be considered with real constants C_1 and C_2 in (1) leading to the angle independent deformation of the sphere, which results in a new sphere with radius $R(1 + C_1\beta + C_2\beta^2)$. This deformation is not only important to compare the results obtained by the perturbation theory with the ones obtained by the Mie theory [70] but also enables to examine the size effect in the perturbation theory for the same type of objects with different sizes. The results are in a very good agreement and not presented here because of this article limitations.

Next, the results can be checked by considering geometries having rotational symmetry obtained by using deformation functions in the form of $f_i(\theta,\varphi) = f_i(\theta)$. A spheroid is one of those type of geometries and it is considered in the analysis of many important problems [69], [71]–[78]. The surface of spheroid is described, as a deformed sphere, by the following relation [77]:

$$r_s(\theta) = R\left(1 - \frac{h^2}{2}\sin^2\theta - \frac{h^4}{2}\left(\sin^2\theta - \frac{3}{4}\sin^4\theta\right)\right). \tag{20}$$

In [77], h^2 is used as a perturbation parameter and it corresponds to the perturbation parameter given as β in (1). Since $\beta = h^2$, the results for prolate and oblate spheroids in [77] can be obtained by $\beta = h^2$ and $\beta = -h^2$, respectively, with $f_1(\theta) = -1/2\sin^2\theta$ and $f_2(\theta) = -1/2\sin^2\theta + 3/8\sin^4\theta$. In Fig. 2, backward RCS (σ_{b}) obtained by the second-order perturbation for prolate spheroids is examined and compared with the ones obtained by CST for various values of h. It is seen that the results are in a good agreement. Bistatic RCS results are also presented in Fig. 3 for a prolate spheroid obtained with $h = 0.4$ at $kR = 1$ and the results are in a very good agreement. By the comparisons given above, it can be concluded that the present results are consistent with the ones obtained by CST for the spheroids.

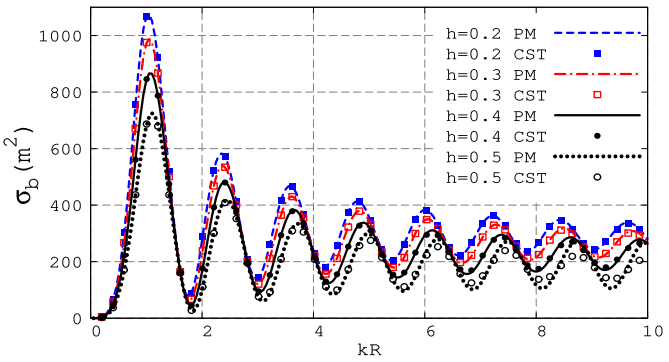

Fig. 2. Backward RCS for prolate spheroids. Comparison of the results obtained by the PM and CST for various h values.

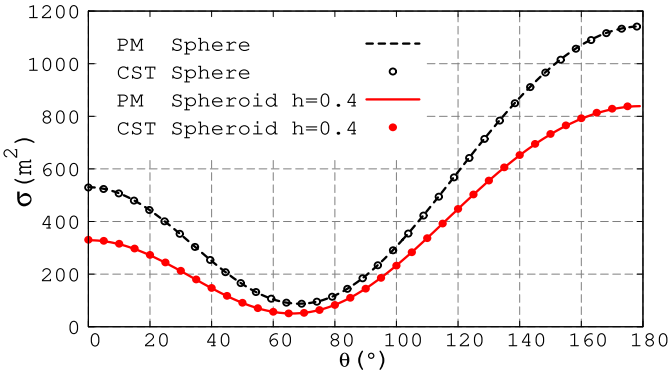

Fig. 3. Bistatic RCS for prolate spheroid $h = 0.4$ and for the sphere at $kR = 1$ with $\varphi = 0$ and $\vec{E}^{\mathrm{i}} = e^{ikz}\hat{x}$.

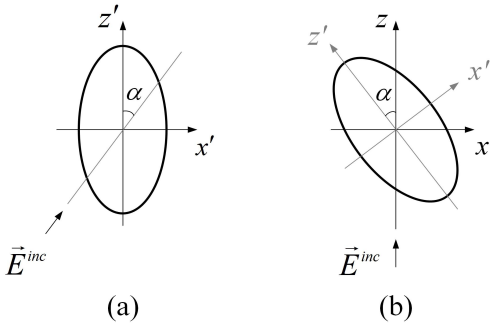

Fig. 4. Coordinate transformation for comparisons. (a) Spheroid. (b) Rotated spheroid by an angle α.

Finally, in the third case, the results are checked by transforming the backward RCS values of a φ independent scatterer under oblique incidence with the ones obtained by CST for spheroids. For comparison purposes, the spheroid examined in [77] as shown in Fig. 4(a) is considered in the primed coordinate system. Employing a rotation by an angle α leads to a θ- and φ-dependent geometry in unprimed coordinate system as shown in Fig. 4(b), which results in θ- and φ-dependent deformation functions $f_1(\theta, \varphi)$ and $f_2(\theta, \varphi)$. With that approach for this very special case, the results of that φ independent geometry are utilized for the comparison and validation of the perturbation results of the θ- and φ-dependent geometry. The deformation functions

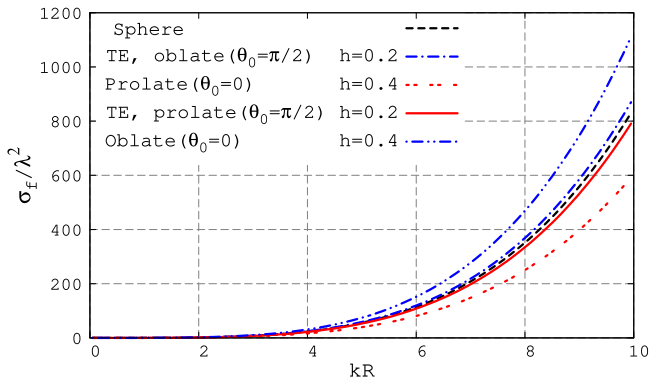

Fig. 5. Normalized forward RCS for prolate and oblate spheroids.

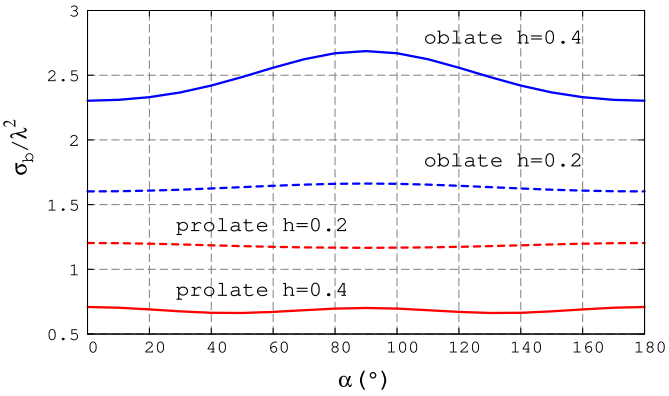

Fig. 6. Normalized backward RCS for prolate and oblate spheroids for TE case.

can also be obtained by using Wigner rotation matrices [79] for that special case. Since the Wigner rotation matrices can be employed for any kind of rotation in 3-D space, the deformation functions can be obtained for any case by their usage and that allows one to examine θ- and φ-dependent geometries for TE or TM incidence without the need of any separate treatment. It is also worth mentioning here that the usage of Wigner rotation matrices in the present work, which allows one to consider 3-D rotations, is very important for detecting buried objects. It is known that for spheroidal targets, there exists some blind orientation that prevents buried objects to be detected [10]. Thus, the present approach allows one to consider different angles of incidence without repeating all of the calculations from the beginning and therefore has the potential to find application in that area. Forward RCS (σ_{f}) results obtained by the second-order perturbation are shown in Fig. 5. Both prolate and oblate spheroids for the deformation parameters 0.2 and 0.4 are considered and it is seen that the results are consistent with [77, Fig. 6]. Moreover, if the backward RCS results presented in Fig. 6 are compared with the ones shown in [77, Fig. 2] where α corresponds to θ_0 of that figure, it can be seen that they are also in a very good agreement.

Consequently, the verification and validation of the results reveal that the methodology presented in this article can be

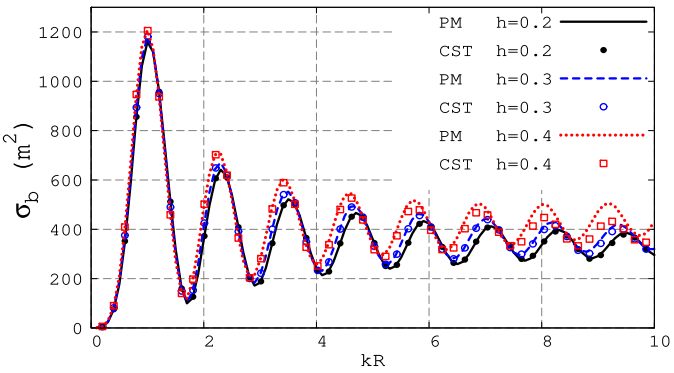

Fig. 7. Backward RCS for triaxial ellipsoid for $\xi = 0.25$ and various values of h with $\vec{E}^{\mathrm{i}} = e^{ikz}\hat{x}$.

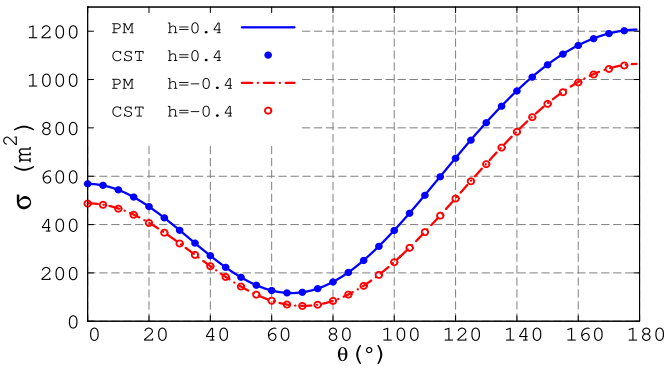

Fig. 8. Bistatic RCS for triaxial ellipsoid for $\xi = 0.25$ and $h = \pm 0.4$ at $kR = 1$ with $\varphi = 0$ and $\vec{E}^{\mathrm{i}} = e^{ikz}\hat{x}$.

successfully used for the accurate calculation of the RCS of arbitrarily shaped scatterers. Ellipsoidal surfaces can be given as a well-known example for these types of shapes. By expressing the semiaxes of the ellipsoid in terms of the perturbation parameter β as a, $a(1+\beta)$ and $a(1+\beta\xi)$, the equation of the ellipsoid, also called triaxial ellipsoid, can be given as

$$\frac{x^2}{a^2} + \frac{y^2}{a^2(1+\beta)^2} + \frac{z^2}{a^2(1+\beta\xi)^2} = 1 \tag{21}$$

and in spherical coordinates, it can also be written as in (1), where R corresponds to the semiminor axis a, $f_1(\theta,\varphi) = \sin^2\theta\sin^2\varphi + \xi\cos^2\theta$, and $f_2(\theta,\varphi) = (3/2)(f_1^2(\theta,\varphi) - f_1(\theta,\varphi) + (\xi - \xi^2)\cos^2\theta)$ such that ξ is arbitrary and $|\beta\xi| < 1$. The coefficients f_j^s, k_j^s, and h_j^s used in the expansions of the perturbation functions presented in (9), (13), and (14) are given in the Appendix for arbitrary ξ. The incident field for the ellipsoids is again $\vec{E}^{\mathrm{i}} = E^{\mathrm{i}}e^{ikz}\hat{x}$ and it is employed via the expansion in (6) as in the previous cases. Fig. 7 shows the backward RCS results of the ellipsoids for $\xi = 0.25$ and various values of h and the results are in good agreement. To reveal the efficiency of the PM method for an ellipsoid, one may compare the CPU times for the PM and CST solutions. Using the values $kR = 1.5$, $\xi = 0.25$, and $h = 0.2$, the PM method needs 557 s and CST needs 1799 s, which leads to a speedup of 3.23 times. In addition to that, the efficiency of the PM method will be very well appreciated if one considers its application for many different values of h. For every different values of h, one needs to repeat the computations requiring the same amount of time with CST. Since the computations with the PM method are performed using a very simple expression given in (19), the computation time for the new value of h is less than 1×10^{-5} s, which does not make any contribution to the total computation time. Therefore, one can conclude that the PM method is the number of values of $h \times 3.23$ times faster than CST. Bistatic RCS results for ellipsoids are also presented in Fig. 8 and it is seen that the results are in a very good agreement.

In addition to the triaxial ellipsoid results, the present calculations allow to evaluate the RCS results for more irregularly shaped obstacles. A specific example for such kind of deformed objects has been presented in Fig. 1 and RCS results

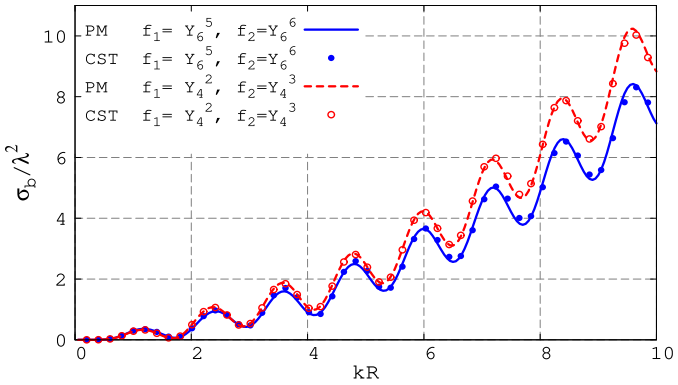

Fig. 9. Normalized backward RCS for the geometries obtained by the deformation function pairs $f_1(\theta,\varphi) = \mathrm{Re}(Y_6^5(\theta,\varphi))$ and $f_2(\theta,\varphi) = \mathrm{Re}(Y_6^6(\theta,\varphi))$ and $f_1(\theta,\varphi) = \mathrm{Re}(Y_4^2(\theta,\varphi))$ and $f_2(\theta,\varphi) = \mathrm{Re}(Y_4^3(\theta,\varphi))$ with $h = 0.36$ and $\vec{E}^{\mathrm{i}} = e^{ikz}\hat{x}$.

for two different cases of that geometry are presented in Fig. 9. Comparisons of the results show the very good agreement and successful implementation of the methodology for irregularly shaped obstacles.

IV. Conclusion

In this study, an analytical solution to the electromagnetic scattering of a plane wave by arbitrarily shaped conducting objects was presented by employing the PM. The geometries of the scatterers are dependent on the θ and φ angles in spherical coordinates, and hence, they have azimuthal variations as well, which increases the complexity significantly, contrary to the ones generally considered with rotational symmetry in the literature. Even though it led to very complicated expressions, second-order corrections were also included in the solutions to obtain more accurate results. Since it is easier to deal with scalar functions, Debye potentials were utilized instead of vector functions. By expanding the deformation functions in terms of spherical harmonics, the scattered field was obtained in terms of Clebsch–Gordan coefficients by evaluating all of the surface integrals analytically and that approach enables one to obtain the results for new geometries without repeating all of the calculations and also eliminates the need of the separate treatment of TE and TM excitations. Scattering results from objects with azimuthal variations including ellipsoids were

also presented. The validations of the results were performed by comparisons with the ones given in the literature accordingly and with the ones obtained by CST. From the results, it can be concluded that the methodology can be successfully employed with high accuracy for the solution to scattering from more irregularly shaped objects.

APPENDIX

The A and B functions with various indices and the results of the integrals involving multiplication of various forms of three associated Legendre functions are presented in the following. The A functions are in the form of $A_\nu = A_\nu(p, j, s, n, m)$ and $A_\nu^q = A_\nu^q(p, q, j, s, n, m)$, the B functions are also in the same form. The arguments of the A and B functions are suppressed in the Appendix for simplicity

$$A_1^q = \frac{qf_j^s a_{0qp}}{\omega\mu\epsilon} r\frac{d}{dr} Z_{2p}(kr) I_0(p, j, n, q, s, m) - \frac{f_j^s b_{0qp}}{\epsilon} r\frac{d}{dr} Z_{3p}(kr) I_4(p, j, n, q, s, m) + \frac{sf_j^s a_{0qp}}{\omega\mu\epsilon} Z_{1p}(kr) I_0(p, j, n, q, s, m) \tag{A.1}$$

$$A_1 = -\frac{f_j^s E^{\mathrm{i}} i^{p+1}}{2} r\frac{d}{dr} j_p(kr)\delta_- \times [I_0(j, p+1, n, s, 1, m) - I_0(j, p-1, n, s, 1, m)] - \frac{sf_j^s E^{\mathrm{i}} i^p (2p+1)}{2} \frac{j_p(kr)}{kr} \times I_0(p, j, n, 1, s, m)\delta_+ \tag{A.2}$$

$$A_2^q = \frac{-sk_j^s a_{0qp}}{2\omega\mu\epsilon} Z_{1p}(kr) I_0(p, j, n, q, s, m) \tag{A.3}$$

$$A_3^q = \frac{sk_j^s a_{0qp}}{2\omega\mu\epsilon} r\frac{d}{dr} Z_{1p}(kr) I_0(p, j, n, q, s, m) \tag{A.4}$$

$$A_4^q = \frac{sf_j^s a_{1qp}}{\omega\mu\epsilon} Z_{1p}(kr) I_0(p, j, n, q, s, m) \tag{A.5}$$

$$A_5^q = \frac{qk_j^s a_{0qp}}{2\omega\mu\epsilon} r^2\frac{d^2}{dr^2} Z_{2p}(kr) I_0(p, j, n, q, s, m) \tag{A.6}$$

$$A_6^q = -\frac{k_j^s b_{0qp}}{2\epsilon} r^2\frac{d^2}{dr^2} Z_{3p}(kr) I_4(p, j, n, q, s, m) \tag{A.7}$$

$$A_7^q = \frac{qf_j^s a_{1qp}}{\omega\mu\epsilon} r\frac{d}{dr} Z_{2p}(kr) I_0(p, j, n, q, s, m) \tag{A.8}$$

$$A_8^q = -\frac{f_j^s b_{1qp}}{\epsilon} r\frac{d}{dr} Z_{3p}(kr) I_4(p, j, n, q, s, m) \tag{A.9}$$

$$A_9^q = \frac{sh_j^s a_{0qp}}{\omega\mu\epsilon} Z_{1p}(kr) I_0(p, j, n, q, s, m) \tag{A.10}$$

$$A_{10}^q = \frac{qh_j^s a_{0qp}}{\omega\mu\epsilon} r\frac{d}{dr} Z_{2p}(kr) I_0(p, j, n, q, s, m) - \frac{h_j^s b_{0qp}}{\epsilon} r\frac{d}{dr} Z_{3p}(kr) I_4(p, j, n, q, s, m) \tag{A.11}$$

$$A_{11} = \frac{sk_j^s E^{\mathrm{i}} i^p (2p+1)}{4} \frac{j_p(kr)}{kr} I_0(p, j, n, 1, s, m)\delta_+ \tag{A.12}$$

$$A_{12} = \frac{-sk_j^s E^{\mathrm{i}} i^p (2p+1)}{4} r\frac{d}{dr}\left(\frac{j_p(kr)}{kr}\right) \times I_0(p, j, n, 1, s, m)\delta_+ \tag{A.13}$$

$$A_{13} = \frac{1}{4} k_j^s E^{\mathrm{i}} i^{p-1} r^2 \frac{d^2}{dr^2} j_p(kr) \times [I_0(p+1, j, n, 1, s, m) - I_0(p-1, j, n, 1, s, m)]\delta_- \tag{A.14}$$

$$A_{14} = -\frac{sh_j^s E^{\mathrm{i}} i^p (2p+1)}{2kr} j_p(kr) I_0(p, j, n, 1, s, m)\delta_+ \tag{A.15}$$

$$A_{15} = \frac{h_j^s E^{\mathrm{i}} i^{p-1}}{2} r\frac{d}{dr} j_p(kr) \times [I_0(p+1, j, n, 1, s, m) - I_0(p-1, j, n, 1, s, m)]\delta_- \tag{A.16}$$

$$B_1^q = -\frac{if_j^s b_{0qp}}{\omega\mu\epsilon} r\frac{d}{dr} Z_{1p}(kr) I_0(p, j, n, q, s, m) + \frac{iqf_j^s a_{0qp}}{\mu} Z_{3p}(kr) I_2(p, j, n, q, s, m) + \frac{if_j^s b_{0qp}}{\omega\mu\epsilon} Z_{2p}(kr) I_1(p, j, n, q, s, m) \times \frac{-isf_j^s a_{0qp}}{\mu} Z_{3p}(kr) I_2(j, p, n, s, q, m) - \frac{isqf_j^s b_{0qp}}{\omega\mu\epsilon} Z_{2p}(kr) I_3(p, j, n, q, s, m) \tag{A.17}$$

$$B_1 = \frac{kf_j^s E^{\mathrm{i}} i^p (2p+1)}{2\omega\mu} r\frac{d}{dr}\left(\frac{j_p(kr)}{kr}\right) I_0(p, j, n, 1, s, m)\delta_- + \frac{kf_j^s E^{\mathrm{i}} i^{p-1}(2p+1)}{2\omega\mu} j_p(kr) \times \left[a_1(p, 0) I_5(j, p+1, n, s, 0, m) + a_2(p, 0) I_5(j, p-1, n, s, 0, m)\right]\delta_- + \frac{skf_j^s E^{\mathrm{i}} i^{p+1}(2p+1)}{2w\mu} j_p(kr) I_6(p, j, n, 0, s, m)\delta_+ \tag{A.18}$$

$$B_2^q = -\frac{ik_j^s b_{0qp}}{2\omega\mu\epsilon} r^2\frac{d^2}{dr^2} Z_{1p}(kr) I_0(p, j, n, q, s, m) \tag{A.19}$$

$$B_3^q = \frac{-if_j^s b_{1qp}}{\omega\mu\epsilon} r\frac{d}{dr} Z_{1p}(kr) I_0(p, j, n, q, s, m) \tag{A.20}$$

$$B_4^q = \frac{iqk_j^s a_{0qp}}{2\mu} r\frac{d}{dr} Z_{3p}(kr) I_2(p, j, n, q, s, m) \tag{A.21}$$

$$B_5^q = \frac{ik_j^s b_{0qp}}{2\omega\mu\epsilon} r\frac{d}{dr} Z_{2p}(kr) I_1(p, j, n, q, s, m) \tag{A.22}$$

$$B_6^q = \frac{iqf_j^s a_{1qp}}{\mu} Z_{3p}(kr) I_2(p, j, n, q, s, m) \tag{A.23}$$

$$B_7^q = \frac{if_j^s b_{1qp}}{\omega\mu\epsilon} Z_{2p}(kr) I_1(p, j, n, q, s, m) \tag{A.24}$$

$$B_8^q = \frac{-iqk_j^s a_{0qp}}{2\mu} Z_{3p}(kr) I_2(p, j, n, q, s, m) \tag{A.25}$$

$$B_9^q = -\frac{ik_j^s b_{0qp}}{2\omega\mu\epsilon} Z_{2p}(kr) I_1(p, j, n, q, s, m) \tag{A.26}$$

$$B_{10}^q = \frac{-isk_j^s a_{0qp}}{2\mu} r\frac{d}{dr} Z_{3p}(kr) I_2(j, p, n, s, q, m) \tag{A.27}$$

$$B_{11}^q = -\frac{isqk_j^s b_{0qp}}{2\omega\mu\epsilon} r \frac{d}{dr} Z_{2p}(kr) I_3(p, j, n, q, s, m) \quad \text{(A.28)}$$

$$B_{12}^q = \frac{-isf_j^s a_{1qp}}{\mu} Z_{3p}(kr) I_2(j, p, n, s, q, m) \quad \text{(A.29)}$$

$$B_{13}^q = -\frac{isqf_j^s b_{1qp}}{\omega\mu\epsilon} Z_{2p}(kr) I_3(p, j, n, q, s, m) \quad \text{(A.30)}$$

$$B_{14}^q = \frac{isk_j^s a_{0qp}}{2\mu} Z_{3p}(kr) I_2(j, p, n, s, q, m) \quad \text{(A.31)}$$

$$B_{15}^q = \frac{isqk_j^s b_{0qp}}{2\omega\mu\epsilon} Z_{2p}(kr) I_3(p, j, n, q, s, m) \quad \text{(A.32)}$$

$$B_{16}^q = \frac{iqh_j^s a_{0qp}}{\mu} Z_{3p}(kr) I_2(p, j, n, q, s, m) + \frac{ih_j^s b_{0qp}}{\omega\mu\epsilon} Z_{2p}(kr) I_1(p, j, n, q, s, m) \quad \text{(A.33)}$$

$$B_{17}^q = -\frac{ish_j^s a_{0qp}}{\mu} Z_{3p}(kr) I_2(j, p, n, s, q, m) - \frac{isph_j^s b_{0qp}}{\omega\mu\epsilon} Z_{2p}(kr) I_3(p, j, n, q, s, m) \quad \text{(A.34)}$$

$$B_{18}^q = -\frac{ih_j^s b_{0qp}}{\omega\mu\epsilon} r \frac{d}{dr} Z_{1p}(kr) I_0(p, j, n, q, s, m) \quad \text{(A.35)}$$

$$B_{19} = \frac{k k_j^s E^{\mathrm{i}} i^p (2p+1)}{4w\mu} r^2 \frac{d^2}{dr^2}\left(\frac{j_p(kr)}{kr}\right) \times I_0(p, j, n, 1, s, m)\delta_- \quad \text{(A.36)}$$

$$B_{20} = -\frac{k k_j^s E^{\mathrm{i}} i^{p+1}(2p+1)}{4w\mu} r \frac{d}{dr} j_p(kr)\delta_- \times [a_1(p,0) I_5(j, p+1, n, s, 0, m) + a_2(p,0) I_5(j, p-1, n, s, 0, m)] \quad \text{(A.37)}$$

$$B_{21} = \frac{k k_j^s E^{\mathrm{i}} i^{p+1}(2p+1)}{4w\mu} j_p(kr)\delta_- \times [a_1(p,0) I_5(j, p+1, n, s, 0, m) + a_2(p,0) I_5(j, p-1, n, s, 0, m)] \quad \text{(A.38)}$$

$$B_{22} = \frac{s k k_j^s E^{\mathrm{i}} i^{p+1}(2p+1)}{4w\mu} r \frac{d}{dr} j_p(kr) \times I_6(p, j, n, 0, s, m)\delta_+ - \frac{s k k_j^s E^{\mathrm{i}} i^{p+1}(2p+1)}{4w\mu} \times j_p(kr) I_6(p, j, n, 0, s, m)\delta_+ \quad \text{(A.39)}$$

$$B_{23} = \frac{k h_j^s E^{\mathrm{i}} i^p (2p+1)}{2w\mu} r \frac{d}{dr}\left(\frac{j_p(kr)}{kr}\right) \times I_0(p, j, n, 1, s, m)\delta_- \quad \text{(A.40)}$$

$$B_{24} = \frac{k h_j^s E^{\mathrm{i}} i^{p-1}(2p+1)}{2w\mu} j_p(kr)\delta_- \times [a_1(p,0) I_5(j, p+1, n, s, 0, m) + a_2(p,0) I_5(j, p-1, n, s, 0, m)] \quad \text{(A.41)}$$

$$B_{25} = \frac{skh_j^s E^{\mathrm{i}} i^{p+1}(2p+1)}{2w\mu} j_p(kr) I_6(p, j, n, 0, s, m)\delta_+ \quad \text{(A.42)}$$

where $a_1(p,q) = ((p-q+1)/(2p+1))$, $a_2(p,q) = ((p+q)/(2p+1))$, $\delta_+ = 2\pi(\delta_{1+s,m} + \delta_{-1+s,m})$, $\delta_- = 2\pi(\delta_{1+s,m} - \delta_{-1+s,m})$, and

$$I_0(p, j, n, q, s, m) = \int_0^\pi P_p^q P_j^s P_n^m \sin\theta d\theta \quad \text{(A.43)}$$

$$I_1(p, j, n, q, s, m) = \int_0^\pi \frac{\partial P_p^q}{\partial\theta}\frac{\partial P_j^s}{\partial\theta} P_n^m \sin\theta d\theta \quad \text{(A.44)}$$

$$I_2(p, j, n, q, s, m) = \int_0^\pi \frac{P_p^q}{\sin\theta}\frac{\partial P_j^s}{\partial\theta} P_n^m \sin\theta d\theta \quad \text{(A.45)}$$

$$I_3(p, j, n, q, s, m) = \int_0^\pi \frac{P_p^q}{\sin\theta}\frac{P_j^s}{\sin\theta} P_n^m \sin\theta d\theta \quad \text{(A.46)}$$

$$I_4(p, j, n, q, s, m) = \int_0^\pi \frac{\partial P_p^q}{\partial\theta} P_j^s P_n^m \sin^2\theta d\theta \quad \text{(A.47)}$$

$$I_5(p, j, n, q, s, m) = \int_0^\pi \frac{\partial P_p^q}{\partial\theta} P_j^s P_n^m \sin\theta d\theta \quad \text{(A.48)}$$

$$I_6(p, j, n, q, s, m) = \int_0^\pi \frac{P_p^q}{\sin\theta} P_j^s P_n^m \sin\theta d\theta \quad \text{(A.49)}$$

where the arguments of the associated Legendre functions, $\cos\theta$, are suppressed for simplicity. The integrals given in (A.44)–(A.48) can be evaluated by transforming them to the expressions involving many integrals similar to (A.43). Considering

$$\frac{d}{dx} P_n^m(x) = \frac{-nx}{1-x^2} P_n^m(x) + \frac{n+m}{1-x^2} P_{n-1}^m(x) \quad \text{(A.50)}$$

$$x P_n^m(x) = \frac{(n-m+1)}{2n+1} P_{n+1}^m(x) + \frac{n+m}{2n+1} P_{n-1}^m(x) \quad \text{(A.51)}$$

$$\frac{P_n^m(x)}{\sqrt{1-x^2}} = (2n-1) P_{n-1}^{m-1}(x) + \frac{P_{n-2}^m(x)}{\sqrt{1-x^2}} \quad \text{(A.52)}$$

and a very useful relation

$$\frac{P_n^m(x)}{\sqrt{1-x^2}} = \sum_{\tau=0}^{\lfloor\frac{n-m}{2}\rfloor} (2(n-2\tau)-1) P_{n-1-2\tau}^{m-1}(x) \quad \text{(A.53)}$$

obtained via (A.52) where $\lfloor x \rfloor$ denotes the greatest integer less or equal to x and those integrals can be written in term of I_0 as

$$\begin{aligned} &I_1(p, j, n, q, s, m) \\ &= \frac{1}{4}[(p-q+1)(p+q) \\ &\quad \times (j-s+1)(j+s) I_0(p, j, n, q-1, s-1, m) \\ &\quad - (p-q+1)(p+q) I_0(p, j, n, q-1, s+1, m) \\ &\quad - (j-s+1)(j+s) I_0(p, j, n, q+1, s-1, m) \\ &\quad + I_0(p, j, n, q+1, s+1, m)] \end{aligned} \quad \text{(A.54)}$$

$$\begin{aligned} &I_2(p, j, n, q, s, m) \\ &= [-\Sigma(p, q, \tau_1)\Sigma(j+1, s, \tau_2) \\ &\quad \times a_3(j, s)\ I_0(p-1-2\tau_1, j-2\tau_2, n, q-1, s-1, m) \\ &\quad - \Sigma(p, q, \tau_3)\Sigma(j-1, s, \tau_4) a_4(j, s) \\ &\quad \times I_0(p-1-2\tau_3, j-2-2\tau_4, n, q-1, s-1, m)] \end{aligned} \quad \text{(A.55)}$$

where $a_3(p,q) = ((-p(p-q+1))/(2p+1))$ and $a_4(p,q) = (((p+q)(p+1))/(2p+1))$

$$I_3(p,j,n,q,s,m) = [\Sigma(p,q,\tau_1)\Sigma(j,s,\tau_2) \times I_0(p-1-2\tau_1, j-1-2\tau_2, n, q-1, s-1, m)] \tag{A.56}$$

$$I_4(p,j,n,q,s,m) = \frac{(p-q+1)(p+q)}{2(2j+1)} \times I_0(p,j+1,n,q-1,s+1,m) - \frac{(p-q+1)(p+q)}{2(2j+1)} I_0(p,j-1,n,q-1,s+1,m) - \frac{1}{2(2j+1)} I_0(p,j+1,n,q+1,s+1,m) + \frac{1}{2(2j+1)} I_0(p,j-1,n,q+1,s+1,m) \tag{A.57}$$

$$I_5(p,j,n,q,s,m) = \frac{1}{2}(p-q+1)(p+q) \times I_0(p,j,n,q-1,s,m) - \frac{1}{2} I_0(p,j,n,q+1,s,m) \tag{A.58}$$

$$I_6(p,j,n,q,s,m) = \Sigma(p,q,\tau) \times I_0(p-2\tau-1, j, n, q-1, s, m) \tag{A.59}$$

where $\Sigma(p,q,\tau)h(p,q,\tau) = \sum_{\tau=0}^{\lfloor((p-q)/2)\rfloor}(2(p-2\tau)-1)h(p,q,\tau)$ for an arbitrary function $h(p,q,\tau)$. The integral I_0 seen in (A.54)–(A.59) and given by (A.43) can be evaluated as [81]

$$\begin{aligned} I_0(p,j,n,q,s,m) &= \int_0^{\pi} P_p^q P_j^s P_n^m \sin\theta d\theta \\ &= \sqrt{\frac{(p+q)!(j+s)!(n+m)!}{(p-q)!(j-s)!(n-m)!}} \left(\sum_{\rho_1=\rho_{1min}}^{p+j} C_{q\,s\,M_2}^{p\,j\,\rho_1} C_{000}^{p\,j\,\rho_1} \right) \\ &\times \left(\sum_{\rho_2=\rho_{2min}}^{\rho_1+n} \sqrt{\frac{(\rho_2-M_3)!}{(\rho_2+M_3)!}} C_{M_2 m M_3}^{\rho_1\,n\,\rho_2} C_{000}^{\rho_1\,n\,\rho_2} \right) \\ &\times \left(\frac{[(-1)^{M_3}+(-1)^{\rho_2}] M_3 2^{M_3-2} \Gamma(\frac{\rho_2}{2}) \Gamma(\frac{\rho_2+M_3+1}{2})}{(\frac{\rho_2-M_3}{2})! \Gamma(\frac{\rho_2+3}{2})} \right) \end{aligned} \tag{A.60}$$

where $C_{m_1 m_2 m_3}^{l_1 l_2 l_3}$ are Clebsch–Gordan coefficients, Γ denotes the Gamma function, $M_2 = q+s$, $M_3 = q+s+m$, $\rho_{1min} = \max(M_2, |p-j|)$, and $\rho_{2min} = \max(M_3, |\rho_1 - n|)$. For the cases where the associated Legendre functions have negative degree and negative order encountered in the evaluation of I_0–I_6 given in (A.43)–(A.49), the integrals are modified by using [30], [66]

$$P_{-n-1}^m(x) = P_n^m(x) \tag{A.61}$$

and

$$P_n^{-m}(x) = (-1)^m \frac{(n-m)!}{(n+m)!} P_n^m(x) \tag{A.62}$$

resulting in additional multiplicative terms in the equations accordingly. The coefficients f_j^s, k_j^s, and h_j^s used in (9), (13), and (14) for ellipsoid are

$$f_0^0 = (1+\xi)/3, \quad f_2^{-2} = -2 \tag{A.63}$$
$$f_2^0 = (-1+2\xi)/3, \quad f_2^2 = -1/12 \tag{A.64}$$
$$k_0^0 = (3+2\xi+3\xi^2)/15, \quad k_2^{-2} = -4(3+\xi)/7 \tag{A.65}$$
$$k_2^0 = 2(-3+\xi+6\xi^2)/21, \quad k_2^2 = -(3+\xi)/42 \tag{A.66}$$
$$k_4^{-4} = 24, \quad k_4^{-2} = \frac{12}{7}(1-2\xi) \tag{A.67}$$
$$k_4^0 = (3-8\xi+8\xi^2)/35, \quad k_4^2 = (1-2\xi)/210 \tag{A.68}$$
$$k_4^4 = 1/1680, \quad h_0^0 = (-1+\xi-\xi^2)/5 \tag{A.69}$$
$$h_2^{-2} = \frac{1}{7}(3-6\xi), \quad h_2^0 = \frac{1}{14}(1+2\xi-2\xi^2) \tag{A.70}$$
$$h_2^2 = \frac{1}{56}(1-2\xi) \tag{A.71}$$
$$h_4^s = 3/2k_4^s \ \ for\ s = -4,-2,0,2,4. \tag{A.72}$$

ACKNOWLEDGMENT

The authors would like to thank Prof. Dr. I. H. Duru for his fruitful discussions. The numerical calculations reported in this article were partially performed at TUBITAK ULAKBIM, High Performance and Grid Computing Center (TRUBA resources). They also thank Mustafa Seçmen, Yaşar University, for his help about CST. They are grateful to the reviewers for their very valuable constructive comments to improve this article.

REFERENCES

[1] C. Fogle, A. C. Rowat, A. J. Levine, and J. Rudnick, "Shape transitions in soft spheres regulated by elasticity," *Phys. Rev. E, Stat. Phys. Plasmas Fluids Relat. Interdiscip. Top.*, vol. 88, no. 5, Nov. 2013, Art. no. 052404.

[2] D. K. Srivastava, R. R. Yadav, and S. Yadav, "Steady Stokes flow around deformed sphere. Class of oblate axisymmetric bodies," *Int. J. Appl. Math. Mech.*, vol. 8, no. 9, pp. 17–53, Jan. 2012.

[3] A. Hobolth, "The spherical deformation model," *Biostatistics*, vol. 4, no. 4, pp. 583–595, Oct. 2003.

[4] M. I. Mishchenko, G. Videen, V. A. Babenko, N. G. Khlebtsov, and T. Wriedt, "T-matrix theory of electromagnetic scattering by particles and its applications: A comprehensive reference database," *J. Quantum Spectrosc. Radiat. Transf.*, vol. 88, pp. 357–406, Aug. 2004.

[5] J. B. Mehl, "Acoustic resonance frequencies of deformed spherical resonators," *J. Acoust. Soc. Amer.*, vol. 71, no. 5, pp. 1109–1113, May 1982.

[6] J. B. Mehl, "Acoustic resonance frequencies of deformed spherical resonators. II," *J. Acoust. Soc. Amer.*, vol. 79, no. 2, pp. 278–286, Feb. 1986.

[7] J. B. Mehl, "Acoustic eigenvalues of a quasispherical resonator: Second order shape perturbation theory for arbitrary modes," *J. Res. Nat. Ins. Stand. Tech.*, vol. 112, no. 3, pp. 163–173, May 2007.

[8] A. Mugnai and W. J. Wiscombe, "Scattering of radiation by moderately nonspherical particles," *J. Atmospheric Sci.*, vol. 37, pp. 1291–1307, Jun. 1980.

[9] R. J. Martin, "Mie scattering formulae for non-spherical particles," *J. Modern Opt.*, vol. 40, no. 12, pp. 2467–2494, Dec. 1993.

[10] P. P. Silvester and D. Omeragic, "Sensitivity of metal detectors to spheroidal targets," *IEEE Trans. Geosci. Remote Sens.*, vol. 33, no. 6, pp. 1331–1335, Nov. 1995.

[11] S. Vitebskiy, K. Sturgess, and L. Carin, "Short-pulse plane-wave scattering from buried perfectly conducting bodies of revolution," *IEEE Trans. Antennas Propag.*, vol. 44, no. 2, pp. 143–151, Feb. 1996.

[12] B. Shanker, A. A. Ergin, K. Aygun, and E. Michielssen, "Analysis of transient electromagnetic scattering from closed surfaces using a combined field integral equation," *IEEE Trans. Antennas Propag.*, vol. 48, no. 7, pp. 1064–1074, Jul. 2000.

[13] S. J. Norton, W. A. SanFilipo, and I. J. Won, "Eddy-current and current-channeling response to spheroidal anomalies," *IEEE Trans. Geosci. Remote Sens.*, vol. 43, no. 10, pp. 2200–2209, Oct. 2005.

[14] J. B. Mehl, "Second-order electromagnetic eigenfrequencies of a triaxial ellipsoid," *Metrologia*, vol. 46, no. 5, pp. 554–559, Oct. 2009.

[15] D. Lyasota, V. M. Morozov, and V. I. Magro, "Recognition of conductive objects based on the characteristics of reflected electromagnetic wave," *Radioelectronics Commun. Syst.*, vol. 59, no. 7, pp. 293–300, Jul. 2016.

[16] Y. Liu, A. C. Yücel, H. Bagci, A. C. Gilbert, and E. Michielssen, "A wavelet-enhanced PWTD-accelerated time-domain integral equation solver for analysis of transient scattering from electrically large conducting objects," *IEEE Trans. Antennas Propag.*, vol. 66, no. 5, pp. 2458–2470, May 2018.

[17] N. L. Tsitsas, G. P. Zouros, G. Fikioris, and Y. Leviatan, "On methods employing auxiliary sources for 2-D electromagnetic scattering by noncircular shapes," *IEEE Trans. Antennas Propag.*, vol. 66, no. 10, pp. 5443–5452, Oct. 2018.

[18] M. Alian and H. Oraizi, "Electromagnetic multiple PEC object scattering using equivalence principle and addition theorem for spherical wave harmonics," *IEEE Trans. Antennas Propag.*, vol. 66, no. 11, pp. 6233–6243, Aug. 2018.

[19] S. Afifi and R. Dusséaux, "Scattering from 2-D perfect electromagnetic conductor rough surface: Analysis with the small perturbation method and the small-slope approximation," *IEEE Trans. Antennas Propag.*, vol. 66, no. 1, pp. 340–346, Jan. 2018.

[20] N. Vojnovic, M. Nikolic Stevanovic, L. Crocco, and A. R. Djordjevic, "High-order sparse shape imaging of PEC and dielectric targets using TE polarized fields," *IEEE Trans. Antennas Propag.*, vol. 66, no. 4, pp. 2035–2043, Apr. 2018.

[21] G. Edwards and R. Underwood, "The electromagnetic fields of a triaxial ellipsoid calculated by modal superposition," *Metrologia*, vol. 48, no. 3, pp. 114–122, Mar. 2011.

[22] J. B. Mehl, "Second-order electromagnetic eigenfrequencies of a triaxial ellipsoid II," *Metrologia*, vol. 52, no. 5, pp. 227–232, Oct. 2015.

[23] D.-P. Lin and H.-Y. Chen, "An empirical formula for the prediction of rain attenuation in frequency range 0.6–100 GHz," *IEEE Trans. Antennas Propag.*, vol. 50, no. 4, pp. 545–551, Apr. 2002.

[24] R. Olsen, D. Rogers, and D. Hodge, "The aR^b relation in the calculation of rain attenuation," *IEEE Trans. Antennas Propag.*, vol. AP-26, no. 2, pp. 318–329, Mar. 1978.

[25] H. R. Pruppacher and R. L. Pitter, "A semi-empirical determination of the shape of cloud and rain drops," *J. Atmos. Sci.*, vol. 28, no. 1, pp. 86–94, Jan. 1971.

[26] L. W. Li, P. S. Kooi, M. S. Leong, and T. S. Yeo, "On the simplified expression of realistic raindrop shapes," *Microw. Opt. Technol. Lett.*, vol. 7, no. 4, pp. 201–205, Mar. 1994.

[27] L.-W. Li, P.-S. Kooi, M.-S. Leong, T.-S. Yee, and M.-Z. Gao, "Microwave attenuation by realistically distorted raindrops: Part II. Predictions," *IEEE Trans. Antennas Propag.*, vol. 43, no. 8, pp. 823–828, Aug. 1995.

[28] L.-W. Li, T.-S. Yeo, P.-S. Kooi, and M.-S. Leong, "An efficient calculational approach to evaluation of microwave specific attenuation," *IEEE Trans. Antennas Propag.*, vol. 48, no. 8, pp. 1220–1229, Aug. 2000.

[29] C. Yeh, "Perturbation approach to the diffraction of electromagnetic waves by arbitrarily shaped dielectric obstacles," *Phys. Rev.*, vol. 135, no. 5A, pp. A1193–A1201, Aug. 1964.

[30] P. M. Morse and H. Feshbach, *Methods of Theoretical Physics*. New York, NY, USA: McGraw-Hill, 1953.

[31] T. Oguchi, "Attenuation of electromagnetic wave due to rain with distorted raindrops," *J. Radio. Res. Lans.*, vol. 7, pp. 467–485, 1960.

[32] R. F. Harrington, *Field Computation by Moment Methods*. New York, NY, USA: IEEE Press, 1987.

[33] K. Umashankar, A. Taflove, and S. Rao, "Electromagnetic scattering by arbitrary shaped three-dimensional homogeneous lossy dielectric objects," *IEEE Trans. Antennas Propag.*, vol. AP-34, no. 6, pp. 758–766, Jun. 1986.

[34] A. C. Ludwig, "The generalized multi pole technique," *Comp. Phys. Com.*, vol. 68, nos. 1–3, pp. 306–314, 1991.

[35] A. Lakhatakia and G. W. Mulholland, "On two numerical techniques for light scattering by dielectric agglomerated structures," *J. Res. Nat. Inst. Standards Technol.*, vol. 98, no. 6, pp. 699–716, Nov. 1993.

[36] K. Yee, "Numerical solution of initial boundary value problems involving Maxwell's equations in isotropic media," *IEEE Trans. Antennas Propag.*, vol. AP-14, no. 3, pp. 302–307, May 1966.

[37] J. L. Volakis, A. Chatterje, and L. C. Kempel, "Review of the finite-element method for three-dimensional electromagnetic scattering," *J. Opt. Soc. Amer. A, Opt. Image Sci.*, vol. 11, no. 4, pp. 1422–1433, 1994.

[38] P. C. Waterman, "Symmetry, unitarity, and geometry in electromagnetic scattering," *Phys. Rev. D, Part. Fields*, vol. 3, no. 4, pp. 825–839, Feb. 1971.

[39] D. Petrov, E. Synelnyk, Y. Shkuratov, and G. Videen, "The T-matrix technique for calculations of scattering properties of ensembles of randomly oriented particles with different size," *J. Quant. Spectrosc. Radiat. Transf.*, vol. 102, no. 1, pp. 85–110, Nov. 2006.

[40] H. Zamani, A. Tavakoli, and M. Dehmollaian, "Scattering from two rough surfaces with inhomogeneous dielectric profiles," *IEEE Trans. Antennas Propag.*, vol. 63, no. 12, pp. 5753–5766, Dec. 2015.

[41] H. Zamani, A. Takavoli, and M. Dehmollaian, "Scattering from layered rough surfaces: Analytical and numerical investigations," *IEEE Trans. Geo. Remote Sens.*, vol. 54, no. 6, pp. 3685–5696, Jun. 2016.

[42] V. A. Erma, "Perturbation approach to the electrostatic problem for irregularly shaped conductors," *J. Math. Phys.*, vol. 4, no. 12, pp. 1517–1526, Dec. 1963.

[43] V. A. Erma, "An exact solution for the scattering of electromagnetic waves from conductors of arbitrary shape. I. Case of cylindrical symmetry," *Phys. Rev.*, vol. 173, no. 5, p. 1243, Sep. 1968.

[44] V. A. Erma, "Exact solution for the scattering of electromagnetic waves from conductors of arbitrary shape. II. General case," *Phys. Rev.*, vol. 176, no. 5, pp. 1544–1553, Dec. 1968.

[45] U. Raval and C. P. Gupta, "Electromagnetic scattering due to deformed inhomogeneous bodies (Part I: Sphere)," *Pure Appl. Geophys.*, vol. 87, no. 1, pp. 134–145, Dec. 1971.

[46] U. Raval and C. P. Gupta, "Electromagnetic scattering due to deformed inhomogeneous bodies (Part II: Cylinder)," *Pure Appl. Geophys.*, vol. 87, no. 1, pp. 146–154, Dec. 1971.

[47] N. C. Skaropoulos and D. P. Chrissoulidis, "On the accuracy of perturbative solutions to wave scattering from rough closed surfaces," *J. Acoust. Soc. Amer.*, vol. 114, no. 2, pp. 726–736, Aug. 2003.

[48] J. T. Johnson, "Third-order small-perturbation method for scattering from dielectric rough surfaces," *J. Opt. Soc. Amer. A, Opt. Image Sci.*, vol. 16, no. 11, pp. 2720–2736, Nov. 1999.

[49] M. A. Demir and J. T. Johnson, "Fourth-and higher-order small-perturbation solution for scattering from dielectric rough surfaces," *J. Opt. Soc. Amer. A, Opt. Image Sci.*, vol. 20, no. 12, pp. 2330–2337, Dec. 2003.

[50] M. A. Demir, J. T. Johnson, and T. J. Zajdel, "A study of the fourth-order small perturbation method for scattering from two-layer rough surfaces," *IEEE Trans. Geosci. Remote Sens.*, vol. 50, no. 9, pp. 3374–3382, Sep. 2012.

[51] J. Wiersig, "Perturbative approach to optical microdisks with a local boundary deformation," *Phys. Rev. A, Gen. Phys.*, vol. 85, no. 6, Jun. 2012, Art. no. 063838.

[52] M. M. White and S. C. Creagh, "Quality factors of deformed dielectric cavities," *J. Phys. A, Math. Theor.*, vol. 45, no. 27, Jun. 2012, Art. no. 275302.

[53] H. Zamani, A. Tavakoli, and M. Dehmollaian, "Second-order perturbative solution of scattering from two rough surfaces with arbitrary dielectric profiles," *IEEE Trans. Antennas Propag.*, vol. 63, no. 12, pp. 5767–5776, Dec. 2015.

[54] H. Zamani, A. Tavakoli, and M. Dehmollaian, "Second-order perturbative solution of cross-polarized scattering from multilayered rough surfaces," *IEEE Trans. Antennas Propag.*, vol. 64, no. 5, pp. 1877–1890, May 2016.

[55] T. Wang, L. Tsang, J. T. Johnson, and S. Tan, "Scattering and transmission of waves in multiple random rough surfaces: Energy conservation studies with the second order small perturbation method," *Prog. Electromagn. Res.*, vol. 157, pp. 1–20, Oct. 2016.

[56] H.-Y. Xie, M.-Y. Ng, and Y.-C. Chang, "Analytical solutions to light scattering by plasmonic nanoparticles with nearly spherical shape and nonlocal effect," *J. Opt. Soc. Amer. A, Opt. Image Sci.*, vol. 27, no. 11, p. 2411, Nov. 2010.

[57] R. Schiffer, "Light scattering by perfectly conducting statistically irregular particles," *J. Opt. Soc. Amer. A, Opt. Image Sci.*, vol. 6, no. 3, pp. 385–402, Mar. 1989.

[58] T. Nousiainen, K. Muinonen, J. Avelin, and A Sihvola, "Microwave backscattering by nonspherical ice particles at 5.6 GHz using second-order perturbation series," *J. Quantum Spect.*, vol. 70, nos. 4–6, pp. 639–661, Aug. 2001.

[59] G. A. Farias, E. F. Vasconcelos, S. L. Cesar, and A. A. Maradudin, "Mie scattering by a perfectly conducting sphere with a rough surface," *Physica A, Stat. Mech. Appl.*, vol. 207, nos. 1–3, pp. 315–322, Jun. 1994.

[60] A. Charalambopoulos and G. Dassios, "Scattering of a spherical wave by a small ellipsoid," *IMA JAM*, vol. 62, pp. 117–136, May 1999.

[61] G. Perrusson, M. Lambert, D. Lesselier, A. Charalambopoulos, and G. Dassios, "Electromagnetic scattering by a triaxial homogeneous penetrable ellipsoid: Low-frequency derivation and testing of the localized nonlinear approximation," *Radio Sci.*, vol. 35, pp. 463–481, Mar. 2000.
[62] G. Perrusson, D. Lesselier, M. Lambert, B. Bourgeois, A. Charalambopoulos, and G. Dassios, "Conductive masses in a half-space earth in the diffusive regime: Fast hybrid modeling of a low-contrast ellipsoid," *IEEE Trans. Geosci. Remote Sens.*, vol. 38, no. 4, pp. 1585–1599, Jul. 2000.
[63] G. D. Kolezas, G. P. Zouros, and J. A. Roumeliotis, "Scattering and radiation by perturbed spherical metallic bodies of revolution," *IEEE Antennas Wireless Propag. Lett.*, vol. 15, pp. 1008–1011, 2016.
[64] D. Sarkar and N. J. Halas, "General vector basis function solution of Maxwell's equations," *Phys. Rev. E, Stat. Phys. Plasmas Fluids Relat. Interdiscip. Top.*, vol. 56, no. 1, pp. 1102–1112, Jul. 1997.
[65] J. A. Stratton, *Electromagnetic Theory*. Newyork, NY, USA: McGraw-Hill, 1941.
[66] G. B. Arfken and H. J. Weber, *Mathematical Methods for Physicist*. Sacramento, CA, USA: Academic, 2015.
[67] H. J. Eom, *Electromagnetic Wave Theory for Boundary Value Problems, an Advanced Course on Analytical Methods*. Berlin, Germany: Springer-Verlag, 2004.
[68] C. A. Balanis, *Advanced Engineering Electromagnetics*. New York, NY, USA: Wiley, 1989.
[69] G. P. Zouros, A. D. Kotsis, and J. A. Roumeliotis, "Electromagnetic scattering from a metallic prolate or oblate spheroid using asymptotic expansions on spheroidal eigenvectors," *IEEE Trans. Antennas Propag.*, vol. 62, no. 2, pp. 839–851, Feb. 2014.
[70] R. F. Harrington, *Time-Harmonic Electromagnetic Fields*. New York, NY, USA: IEEE Press, 2001.
[71] Y. Mushiake, "Backscattering for arbitrary angles of incidence of a plane electromagnetic wave on a perfectly conducting spheroid with small eccentricity," *J. Appl. Phys.*, vol. 27, no. 12, pp. 1549–1556, Dec. 1956.
[72] L. W. Li, X. K. Kang and M. S. Leong, *Spheroidal Wave Functions in Electromagnetic Theory*. Newyork, NY, USA: Wiley, 2002.
[73] G. C. Kokkorakis and J. A. Roumeliotis, "Electromagnetic eigenfrequencies in a spheroidal cavity," *J. Electromagn. Waves Appl.*, vol. 11, no. 3, pp. 279–292, Jan. 1997.
[74] G. S. Zalevsky, A. V. Muzychenko, and O. I. Sukharevsky, "Method of radar detection and identification of metal and dielectric objects with resonant sizes located in dielectric medium," *Radioelectronics Commun. Syst.*, vol. 55, no. 9, pp. 393–404, Sep. 2012.
[75] G. P. Zouros, A. D. Kotsis, and J. A. Roumeliotis, "Efficient calculation of the electromagnetic scattering by lossless or lossy, prolate or oblate dielectric spheroids," *IEEE Trans. Microw. Theory Techn.*, vol. 63, no. 3, pp. 864–876, Mar. 2015.
[76] G. P. Zouros, G. D. Kolezas, and J. A. Roumeliotis, "Fast solution of the electromagnetic scattering by composite spheroidal–spherical and spherical–spheroidal configurations," *IEEE Trans. Microw. Theory Techn.*, vol. 63, no. 10, pp. 3042–3053, Oct. 2015.
[77] A. D. Kotsis and J. A. Roumeliotis, "Electromagnetic scattering by a metallic spheroid using shape perturbation method," *Prog. Electromagn. Res.*, vol. 67, pp. 113–134, 2007.
[78] G. D. Kolezas, G. P. Zouros, and K. L. Tsakmakidis, "Engineering subwavelength nanoantennas in the visible by employing resonant anisotropic nanospheroids," *IEEE J. Sel. Topics Quantum Electron.*, vol. 25, no. 3, pp. 1–12, May 2019.
[79] M. Elwenspoek, "Theory of light scattering from aspherical particles of arbitrary size," *J. Opt. Soc. Amer.*, vol. 72, no. 6, pp. 747–755, Jun. 1982.
[80] M. de Podesta *et al.*, "Characterization of the volume and shape of quasi-spherical resonators using coordinate measurement machines," *Metrologia*, vol. 47, no. 5, pp. 588–604, Sep. 2010.
[81] S.-H. Dong and R. Lemus, "The overlap integral of three associated legendre polynomials," *Appl. Math. Lett.*, vol. 15, no. 5, pp. 541–546, Jul. 2002.